

## Autodetachment spectroscopy of vibrationally excited acetaldehyde enolate anion, $\text{CH}_2\text{CHO}^-$

Amy S. Mullin, Kermit K. Murray<sup>1</sup>, C.P. Schulz<sup>2</sup>, Diane M. Szaflarski<sup>3</sup> and W.C. Lineberger

*Joint Institute for Laboratory Astrophysics, University of Colorado and National Institute of Standards and Technology  
and Department of Chemistry and Biochemistry, University of Colorado, Boulder, CO 80309-0440, USA*

Received 12 February 1992; in final form 3 June 1992

The autodetachment spectrum of acetaldehyde enolate anion,  $\text{CH}_2\text{CHO}^-$ , is recorded near  $14180\text{ cm}^{-1}$  using a coaxial laser-ion threshold photodetachment spectrometer. The spectrum represents transitions from  $v=1$  in the  $\nu_3$  C–C–O bending mode of  $\text{CH}_2\text{CHO}^-$  to  $v=0$  in the autodetaching dipole-bound state of the anion. The 32 rotationally resolved (0, 1) hot band transitions reported here were fit to Watson's A-reduced Hamiltonian in conjunction with the previously reported (0, 0) transitions. Rotational constants for  $\nu_3$ ,  $v=1$  of the ground electronic state are determined to be  $A=2.782(2)\text{ cm}^{-1}$ ,  $B=1.3619(4)\text{ cm}^{-1}$ , and  $C=0.3147(4)\text{ cm}^{-1}$ . The (0, 1) band origin is  $14186.928(8)\text{ cm}^{-1}$ , which places  $\omega_0$  for the  $\nu_3$  mode at  $525.82(1)\text{ cm}^{-1}$ .

### 1. Introduction

The determination of the detailed structure and energetics of molecular ions poses a substantial challenge to spectroscopists. The low number densities and high chemical reactivity of gas phase ions can make the usual methods of direct absorption [1–3] spectroscopy difficult. In the last twenty years, a number of alternate techniques have emerged for the spectroscopic study of ions. Among these are modulated absorption [4,5] in electrical discharges, laser magnetic resonance [6] FTIR [7], direct absorption in ion beams [8] and laser-ion beam techniques which rely on molecular processes such as charge transfer [9], predissociation [10,11] or autodetachment [12]. Autodetachment and velocity modulated absorption studies have been especially fruitful in obtaining high resolution spectra data on negative

ions. However, studies of the low frequency ( $400\text{--}600\text{ cm}^{-1}$ ) vibrational modes in negative ions are often not amenable to IR absorption since tunable lasers do not continuously span this region at present. In such cases, autodetachment spectroscopy of vibrationally excited negative ions can be used to investigate low frequency vibrational motion.

Negative molecular ions typically have electron affinities of several eV or less, often resulting in only one bound electronic state. Photodetachment of such ions is usually limited to bound-free transitions where detailed rotational and vibrational information on the ion may be obscured. In some cases, however, negative ions can support excited electronic states which autodetach to form a neutral and an unbound electron, thereby providing the possibility of bound-quasibound transitions which can be investigated by high resolution spectroscopic methods. Dipole-bound states [12–15] represent a special type of weakly bound ( $5\text{--}100\text{ cm}^{-1}$ ) excited negative ion state which can exist when the neutral species possesses a dipole moment of  $\approx 2$  debye or greater. In such a state, the excited electron is in a very diffuse orbital located beyond the positive end of the molecular dipole. With sufficient rotational and vibrational excitation in the excited state, it is possible for the negative ion to autodetach via a rotation-electronic coupling mecha-

*Correspondence to:* W.C. Lineberger, Joint Institute for Laboratory Astrophysics, University of Colorado, Boulder, CO 80309-0440, USA.

<sup>1</sup> Present address: Department of Chemistry, Texas A & M University, College Station, TX 77843, USA.

<sup>2</sup> Present address: Fakultät für Physik, Universität Freiburg, Hermann-Herder-Strasse 3, W-7800 Freiburg, Germany.

<sup>3</sup> Present address: Naval Ocean Systems Center, Code 553, 271 Catalina Blvd., San Diego, CA 92152-5000, USA.

nism. Rotationally resolved autodetachment spectra have been obtained for the dipole-bound states of  $\text{CH}_2\text{CHO}^-$  [14],  $\text{CH}_2\text{CFO}^-$  [15],  $\text{CH}_2\text{CN}^-$  [16] and  $\text{FeO}^-$  [17].

Details of the binding and autodetachment dynamics have a significant effect on the observed autodetachment spectrum. The dipole-bound state of acetaldehyde enolate anion [14],  $\text{CH}_2\text{CHO}^-$ , is bound by  $\approx 5 \text{ cm}^{-1}$ . Rotational levels with energies below this binding energy are stable and will not be observed in the autodetachment spectrum. In  $\text{CH}_2\text{CHO}^-$ , autodetachment from rotational levels  $J_{K_a K_c} = 3_{03}$  and below does not occur. Additionally, autodetachment from levels with either  $J > 7$  or  $K_a > 1$  occurs very rapidly [14], resulting in the broadening of lines to the point where they would not be observable, with the present signal to noise levels. While levels with  $K_a > 1$  may be lower in energy than levels which result in narrow lines, rotational motion around the  $a$ -axis is especially efficient at decoupling the extra electron from the molecule's dipole moment, resulting in fast autodetachment.

In this paper, the autodetachment spectrum of vibrationally excited acetaldehyde enolate anion,  $\text{CH}_2\text{CHO}^-$ , is reported. The 32 rotational transitions arise from the  $\nu = 1$  level of the  $\nu_3$  C–C–O bending mode in the ground state anion, and terminate on the  $\nu = 0$  level of the autodetaching dipole-bound state of acetaldehyde enolate anion. The (0, 0) band has been reported [14] previously, along with a detailed spectroscopic analysis and linewidth measurements which correspond to autodetachment lifetimes. In this work, we focus on the vibrational structure of the ground electronic state of acetaldehyde enolate anion. The vibrational frequency and rotational constants for the  $\nu_3$   $\nu = 1$  level are reported. The  $\nu = 1$  rotational constants and the (0, 1) band origin are determined by simultaneously fitting data for the (0, 0) and (0, 1) bands and optimizing the associated nine rotational constants and two band origins in a non-linear least squares fit. Comparison of the inertial defects for the  $\nu = 0$  and  $\nu = 1$  levels provides insight into the “floppiness” of the C–C–O bend in the ground state anion.

## 2. Experimental techniques

The coaxial laser-ion threshold photodetachment spectrometer used in this study has been described in detail previously [14,18]. A mass-selected ion beam is merged coaxially with the output of a single mode tunable ring dye laser, and the photodetachment spectrum is obtained by collecting the photodetached electrons as a function of photon energy and applying the appropriate normalization. Ion source conditions such as pressure and extraction voltage are chosen to optimize production of the vibrationally excited ions. Specifically, a 2–3 nA beam of acetaldehyde enolate anion is formed by extracting negative ions from a hot-cathode electric discharge which contains  $\approx 0.4$  Torr of an acetaldehyde and  $\text{N}_2\text{O}$  mixture. Ions with mass to charge ratio  $m/q = 43$  are mass selected using a  $90^\circ$  magnet, accelerated to 2.2 keV and merged coaxially with the laser beam in a 30 cm interaction region using electrostatic quadrupole deflectors. Detached electrons are collected by means of a weak magnetic field ( $\approx 5 \text{ G}$ ) which guides the low-energy threshold electrons into an electron multiplier. At the exit of the interaction region, the enolate ions and the neutral photodetachment products are separated by a second quadrupole deflector. The fast neutral beam passes through the deflector and impinges on a glass plate where secondary electrons are ejected and may be collected. The parent ion beam is deflected with the quadrupole into a Faraday cup, where the ion current is monitored.

A tunable home built cw ring dye laser using pyridine-1 dye (690–800 nm) is operated single mode with 10 MHz resolution. Output powers of 250 mW are obtained when pumped with 5–6 W from all lines of an argon ion laser. Wavelength measurements to within  $0.01 \text{ cm}^{-1}$  are made with a traveling Michelson interferometer [19]. The overall resolution of the spectrometer is governed by the energy spread and angular divergence of the ion beam and the bandwidth of the laser, and for these studies is  $\approx 40 \text{ MHz}$ , with the major contribution to the instrument resolution arising from the initial ion energy spread in the ion source.

Laser frequency scanning and data collection are controlled by a computer which scans the laser and simultaneously monitors the electron count rate, laser power and ion current. The spectra are collected by

stepping the laser 25 MHz with a 2 second integration time per step. Autodetachment resonances result in 4 kHz electron signal on top of 3.5 kHz from direct detachment. Scans are collected in  $2.5 \text{ cm}^{-1}$  increments, normalized to laser power and ion current and spliced together. The experimentally determined photon energy is Doppler corrected by  $\approx 5 \text{ cm}^{-1}$  to yield the photon energy absorbed by the ion beam.

### 3. Spectral assignment

The autodetachment spectrum of vibrationally excited acetaldehyde enolate anion is presented here. Ions in the ground  $A'$  electronic state are photoexcited to a dipole-bound electronic state with  $A''$  symmetry. This excited state can rapidly decay to produce an electron and a neutral molecule. The ground electronic anion state is thermally populated with one quantum in the C–C–O  $\nu_3$  bending vibration. In previous lower resolution ( $\approx 1 \text{ cm}^{-1}$ ) photodetachment [14] studies of acetaldehyde enolate anion, a rotationally unresolved peak was observed at  $14185 \text{ cm}^{-1}$ , as shown in fig. 1, and assigned as the C–C–O bending (0, 1) hot band. In the data shown in fig. 1, the resonance features (resonances which produce slow electrons) are greatly enhanced in the threshold elec-

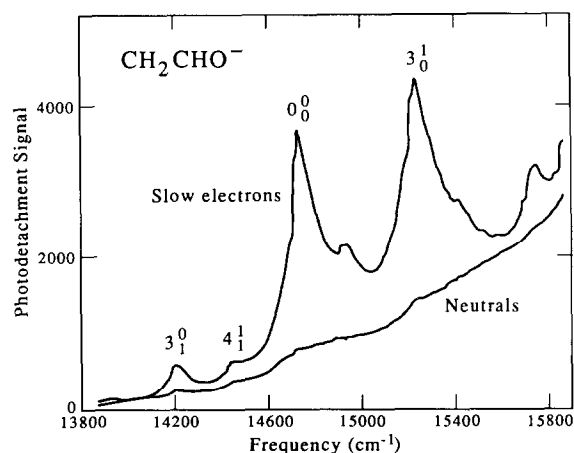


Fig. 1. Photodetachment cross section of  $\text{CH}_2\text{CHO}^-$  taken with  $1 \text{ cm}^{-1}$  resolution (from ref. [12]) where  $\nu_3$  is the CCO bend and  $\nu_4$  is the torsional mode. The  $3_1^0$  bending hot band is investigated under high resolution in this study.

tron cross section data, while the neutral molecule production curve reflects the *total* photodetachment cross section. Upon investigation with higher resolution ( $40 \text{ MHz}$ ), 32 rotationally resolved lines were observed in the autodetachment spectrum from  $14160$  to  $14200 \text{ cm}^{-1}$ . A  $13 \text{ cm}^{-1}$  portion of the spectrum is shown in fig. 2a, where rotationally resolved structure is clearly present. An expanded view of the spectrum between  $14184.6$  and  $14185.1 \text{ cm}^{-1}$  is shown in fig. 2b and illustrates the broadening in the autodetachment resonances as the rotational energy increases. The rotational linewidths correspond to autodetachment lifetimes of the dipole-bound state and should be identical to those reported for the (0, 0) band since the two vibrational transitions share a common upper state. The initial rotational assignments were made in conjunction with the (0, 0) data using combination differences to identify pairs of

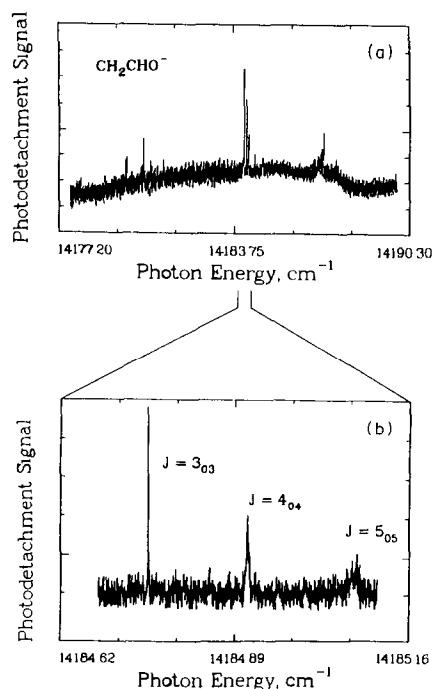


Fig. 2. (a) High resolution scan ( $0.001 \text{ cm}^{-1}$ ) from  $14177$  to  $14190 \text{ cm}^{-1}$  of the  $\text{CH}_2\text{CHO}^-$  autodetachment (0, 1) band. Resonances represent transitions from the vibrationally excited ground state anion to a short-lived dipole-bound state which autodetaches to form a neutral and an unbound electron. (b) Expanded view showing the  $K_a=0 \leftarrow K_a=1$  Q branch. Rapid linewidth broadening occurs as the rotational angular momentum of the upper state increases.

transitions with identical upper state energy spacings. Predictions were generated from these initial estimates and eventually all the observed lines were assigned. The rotational state dependence of the linewidths also helped identify the upper rotational level of each transition. The rotational state assignments, the observed and calculated line positions, and the associated residuals are shown in table 1. Acetaldehyde enolate anion is a near-prolate asymmetric top [14] and its rotational transitions are identified with upper and lower state levels labeled by  $J_{K_a K_c}$ . Only transitions with  $\Delta K_a = \pm 1$  are observed since  $\text{CH}_2\text{CHO}^-$  is just slightly asymmetric. (The asym-

metry parameter for the neutral vinoxy radical is  $\kappa = -0.94$  [20].)

The rotational energy levels of  $\text{CH}_2\text{CHO}^-$  are well described by the Hamiltonian for a near-prolate asymmetric top [21]. The energy levels of an asymmetric rotor are determined here by expanding the asymmetric top wavefunctions using a prolate top basis. For each  $J$  value, the matrix containing interactions between different  $K_a$  states is diagonalized. Since only low  $J$  levels are observed, centrifugal distortion terms are not significant and the  $A$ ,  $B$  and  $C$  rotational constants are sufficient to describe the energy levels.

Table 1

Doppler corrected line positions and residuals ( $\text{cm}^{-1}$ ) for the  $\nu_3$  (0, 1) in the autodetachment spectrum of acetaldehyde enolate anion. Energy levels are labeled by  $J_{K_a K_c}$ . Absolute line positions are accurate to  $\pm 0.01 \text{ cm}^{-1}$ . All lines are given equal weight in the fit

Assignment		Frequency ( $\text{cm}^{-1}$ )		
upper state	lower state	observed	calculated	residuals
5 <sub>15</sub>	6 <sub>25</sub>	14174.83	14174.842	-0.012
6 <sub>15</sub>	7 <sub>25</sub>	14175.17	14175.191	-0.021
4 <sub>14</sub>	5 <sub>24</sub>	14175.55	14175.561	-0.011
5 <sub>14</sub>	6 <sub>24</sub>	14175.63	14175.626	0.004
4 <sub>13</sub>	5 <sub>23</sub>	14176.10	14176.092	0.008
3 <sub>13</sub>	4 <sub>23</sub>	14176.27	14176.271	-0.001
5 <sub>13</sub>	5 <sub>23</sub>	14178.88	14178.875	0.005
4 <sub>12</sub>	4 <sub>22</sub>	14178.94	14178.932	0.008
3 <sub>11</sub>	3 <sub>21</sub>	14178.98	14178.973	0.007
6 <sub>06</sub>	7 <sub>16</sub>	14179.45	14179.434	0.016
4 <sub>13</sub>	4 <sub>23</sub>	14179.50	14179.498	0.002
5 <sub>14</sub>	5 <sub>24</sub>	14179.72	14179.731	-0.011
6 <sub>15</sub>	6 <sub>25</sub>	14180.04	14180.008	0.032
5 <sub>05</sub>	6 <sub>15</sub>	14180.18	14180.191	-0.011
4 <sub>04</sub>	5 <sub>14</sub>	14180.93	14180.930	0.000
3 <sub>03</sub>	3 <sub>13</sub>	14184.77	14184.739	0.032
4 <sub>04</sub>	4 <sub>14</sub>	14184.92	14184.901	0.019
5 <sub>05</sub>	5 <sub>15</sub>	14185.08	14185.096	-0.016
6 <sub>17</sub>	7 <sub>07</sub>	14185.15	14185.127	0.022
6 <sub>06</sub>	6 <sub>16</sub>	14185.29	14185.319	-0.029
5 <sub>16</sub>	6 <sub>06</sub>	14185.50	14185.492	0.008
4 <sub>15</sub>	5 <sub>05</sub>	14185.91	14185.913	-0.003
4 <sub>02</sub>	3 <sub>12</sub>	14187.21	14187.228	-0.018
5 <sub>03</sub>	4 <sub>13</sub>	14187.86	14187.885	-0.025
6 <sub>04</sub>	5 <sub>14</sub>	14188.52	14188.522	-0.002
6 <sub>16</sub>	6 <sub>06</sub>	14188.66	14188.661	-0.001
5 <sub>15</sub>	5 <sub>05</sub>	14188.69	14188.695	-0.005
4 <sub>14</sub>	4 <sub>04</sub>	14188.73	14188.727	0.003
3 <sub>13</sub>	3 <sub>03</sub>	14188.75	14188.755	-0.005
4 <sub>13</sub>	3 <sub>03</sub>	14191.98	14191.982	-0.002
5 <sub>14</sub>	4 <sub>04</sub>	14192.90	14192.897	0.003
6 <sub>15</sub>	5 <sub>05</sub>	14193.87	14193.861	0.009

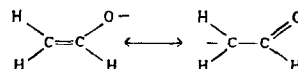
#### 4. Spectral fitting

The 32 lines of the (0, 1) band were initially fit to Watson's *A*-reduced [22] Hamiltonian using a non-linear least squares routine for determination of the upper and lower state molecular constants and the band origin. The results of this fit are shown in table 2, along with the fit reported previously for the (0, 0) band [14]. While the upper state constants from the (0, 1) fit have somewhat higher uncertainty due to the absence of upper state  $K_a > 1$  levels, they are consistent with the values from the (0, 0) fit and confirm that both bands share a common upper state. This permits the (0, 0) and (0, 1) data to be combined in a three state fit, with all lines weighted equally. The results of this fit are also shown in table 2. The final molecular constants for the common upper state now have smaller uncertainty than previously determined and are within the error limits of the initial (0, 0) fit. The overall standard deviation of the fit is  $0.015 \text{ cm}^{-1}$ , which is within the approximate error in the wavelength measurements. Subtracting the two band origins yields an anion vibra-

tional frequency for the C-C-O bend of  $\omega_0 = 525.82(1) \text{ cm}^{-1}$ .

#### 5. Molecular structure

Acetaldehyde enolate anion can be described qualitatively by the following two resonance forms:



As determined in the previous study [14] of the (0, 0) band, acetaldehyde enolate anion is planar in both the anion ground state and the dipole-bound state. The observed transitions between asymmetry doublets in the (0, 0) and (0, 1) bands are consistent with electronic structure calculations [23] which result in  $A'$  symmetry for the ground state and  $A''$  symmetry for the dipole-bound state. The geometry and principal axes of the ground state anion in the vibrationless state were determined earlier [14] using spectra from two isotopic variants. These are shown in fig. 3 along with the direction of the dipole mo-

Table 2

Molecular constants ( $\text{cm}^{-1}$ ) for the ground electronic state ( $\nu_3=0, 1$ ) and the dipole-bound electronically excited state ( $\nu=0$ ) of acetaldehyde enolate anion,  $\text{CH}_2\text{CHO}^-$ . Constants are given for fits involving two states and three states. The preferred data are those resulting from the three state fit

	Constant	(0, 0) fit <sup>a)</sup>	(0, 1) fit	Three state fit
dipole-bound state	<i>A</i>	2.219(3)	2.225(7)	2.221(2)
	<i>B</i>	0.3758(4)	0.3759(5)	0.3759(3)
	<i>C</i>	0.3207(3)	0.3198(5)	0.3204(3)
	<i>A</i> <sup>b)</sup>	0.11(8)		0.18(8)
anion X <sup>1</sup> A'' ( $\nu_3=1$ )	<i>A</i>		2.782(2)	2.782(2)
	<i>B</i>		0.3617(4)	0.3619(4)
	<i>C</i>		0.3145(5)	0.3147(4)
	<i>A</i> <sup>b)</sup>			0.93(8)
anion X <sup>1</sup> A'' ( $\nu_3=0$ )	<i>A</i>	2.493(1)		2.494(1)
	<i>B</i>	0.3622(3)		0.3620(3)
	<i>C</i>	0.3159(4)		0.3159(4)
	<i>A</i> <sup>b)</sup>	0.06(7)		0.04(7)
summary	$\nu_0(0, 0)$	14712.742(5) <sup>c)</sup>		14712.747(5)
	$\nu_0(0, 1)$		14186.93(1)	14186.928(8)
	$\omega_0$			525.82(1)
	$\sigma$	0.014	0.016	0.015

<sup>a)</sup> From ref. [12].

<sup>b)</sup> The inertial defect has units of  $\text{amu} \text{ \AA}^2$ .

<sup>c)</sup> The uncertainty previously reported as  $0.05 \text{ cm}^{-1}$  should be  $0.005 \text{ cm}^{-1}$ .

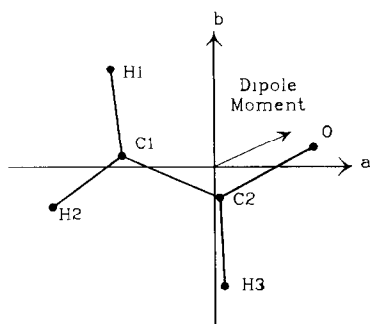


Fig. 3. Structure, principal axes, and dipole moment of the ground vibrationless state of acetaldehyde enolate anion, as determined in ref. [12]. Excitation of  $\nu=1$  in the CCO bend results in substantial opening of the CCO bond angle from  $129^\circ$  to  $136^\circ$ .

ment. The C–C and C–O bond lengths and the C–C–O bond angle were fitted [14] using the molecular constants while the C–H bond lengths and C–C–H bond angles were fixed at values based on measurements for neutral species with similar electronic structure. The resulting structure for the ground state anion in  $\nu=0$  has a C–C bond length of 1.32 Å, very similar to the 1.34 Å length of the double bond in ethylene [21]. The C–O bond length is 1.33 Å which is midway between a single C–O bond in methanol [24] (1.43 Å) and a double C–O bond in formaldehyde [21] (1.21 Å). This illustrates the charge localization of the extra electron on the oxygen atom in the anion ground state. The resulting C–C–O bond angle for the vibrationless anion state is  $129.4^\circ$ .

While the exact determination of molecular structure and vibrational motion requires calculation of the force field, the molecular constants for the  $\nu=1$  level of  $\nu_3$  provide insight into the effect of the bending motion on the anion structure. Using the bond lengths and angles for the vibrationless state and allowing only the C–C–O bond angle to vary, one finds that the C–C–O vibrationally-averaged bond angle must be opened from  $129.4^\circ$  and  $136.4^\circ$  in order to reproduce approximately the experimentally observed constants for the  $\nu_3$   $\nu=1$  state. This large increase in the bond angle suggests that the C–C–O bending potential is quite anharmonic and becomes softer as the bond angle is opened. In comparison, the vinoxy radical has a bending frequency [20]  $\nu_3=496\text{ cm}^{-1}$  with a  $19\text{ cm}^{-1}$  anharmonicity. The anion C–C–O bond angle ( $129.4^\circ$ ) is substantially

greater than that of the neutral analog ( $121.9^\circ$ ). When the electronic structure of the anion is considered, it is reasonable that the bending potential should relax toward larger bond angles, since the diffuse orbital of the extra electron on the oxygen atom will tend to move away from the electron density of the C–H bond on the  $\alpha$ -carbon.

The lack of rigidity in the vibrationally excited ground state is further illustrated by considering the inertial defect of the  $\nu=1$  state. The inertial defect of a molecule is a measure of non-planarity [25] and large amplitude motion, and is given by

$$\Delta \propto \frac{1}{C} - \frac{1}{B} - \frac{1}{A}, \quad (1)$$

where  $A$ ,  $B$ , and  $C$  are the molecular rotational constants. While rigid planar species have  $\Delta=0$ , zero-point vibration causes slightly positive deviations with  $\Delta$  values for many non-linear triatomics ranging [25] from 0 to  $0.2\text{ amu \AA}^2$ . Negative values of  $\Delta$  are indicative of non-planar species. The inertial defects for acetaldehyde enolate anion are given in table 2. The vibrationless ground state has  $\Delta_{\nu_3=0}=0.04(7)$  while in  $\nu=1$  of the bend, we find  $\Delta_{\nu_3=1}=0.93(8)$ . The origin of this large change in  $\Delta$  can be understood as follows. In general, the observed inertial defect is described as the sum of a vibrational, an electronic, and a centrifugal distortion component [25] with

$$\Delta = \Delta_{\text{vib}} + \Delta_{\text{elec}} + \Delta_{\text{cent}}. \quad (2)$$

The large difference between  $\Delta_{(\nu_3=0)}$  and  $\Delta_{(\nu_3=1)}$  is primarily a result of the vibrational term. The electronic contribution will not be significant because the  $\nu=0$  and  $\nu=1$  levels have the same electronic structure and  $\Delta_{\text{cent}}$  should be small since centrifugal distortion terms are not required to fit the transitions of the  $(0,1)$  band within experimental precision. The overall vibrational contribution to the inertial defect is given by [25]

$$\Delta_{\text{vib}} = \sum_s \Delta_s \left( \nu_s + \frac{1}{2} \right), \quad (3)$$

where the  $\nu_s$  values are the quanta of the  $\nu_s$  vibrational mode and the individual  $\Delta_s$  values depend on the vibrational frequencies and the Coriolis coupling constant for the molecule. The Coriolis coupling constants for stretching vibrations are generally small since the displacement of the atoms is nearly along

the bond directions. Large amplitude bending vibrations, however, have larger Coriolis coupling terms and, therefore, have more effect on the inertial defect.

## 6. Conclusions

The autodetachment spectrum for vibrationally excited acetaldehyde enolate anion is reported and assigned. The molecular constants for the C–C–O bending mode are determined by fitting the (0, 1) data in conjunction with the previously reported (0, 0) data and are reported as  $A=2.782(2)$ ,  $B=0.3617(4)$ , and  $C=0.3147(4)$   $\text{cm}^{-1}$ . The (0, 1) band origin is  $14186.928(8)$   $\text{cm}^{-1}$ , which places the  $\nu_3$  bending frequency at  $\omega_0=525.82(1)$   $\text{cm}^{-1}$ . The large change in the  $A$  constant between  $\nu=0$  and  $\nu=1$  in the ground state anion is a consequence of a dramatic opening in the C–C–O bond angle ( $\approx 7^\circ$ ). The inertial defect for the  $\nu=1$  state suggests that large amplitude motion is associated with this state. The C–C–O bending potential appears to become substantially looser as the vibrational energy is increased. This is explained as a result of the diffuse electron cloud on the negatively-charged oxygen being repelled by the electron density of the C–H bond of the  $\alpha$ -carbon.

## Acknowledgement

We thank C.M. Lovejoy and A. McIlroy for their generous sharing of the code for asymmetric top rotational energy levels and R. Parson for many insightful discussions on molecular vibrations. This work was supported by NSF Grants CHE88-19444 and PHY90-12244.

## References

- [1] R.C. Woods, T.A. Dixon, R.J. Saykally and P.G. Szanto, *Phys. Rev. Letters* 35 (1975) 1269.
- [2] R.J. Saykally, T.A. Dixon, T.G. Anderson, P.G. Szanto and R.C. Woods, *Astrophys. J. Letters* 205 (1976) L101.
- [3] T. Oka, *Phys. Rev. Letters* 45 (1980) 531.
- [4] M.H. Begelman, C.S. Gudeman, J. Pfaff and R.J. Saykally, *Phys. Rev. Letters* 51 (1983) 554; J.C. Owruksy, N.H. Rosenbaum, L.M. Tack and R.J. Saykally, *J. Chem. Phys.* 83 (1985) 5338.
- [5] S.C. Foster and A.R.W. McKellar, *J. Chem. Phys.* 81 (1984) 3424.
- [6] R.J. Saykally and K.M. Everson, *Phys. Rev. Letters* 43 (1979) 515; D. Ray, K.G. Kubic and R.J. Saykally, *Mol. Phys.* 46 (1982) 217.
- [7] J.W. Brault and S.P. Davies, *Physica Scripta* 25 (1982) 268.
- [8] E.R. Keim, M.L. Polak, J.C. Owruksy, J.V. Coe and R.J. Saykally, *J. Chem. Phys.* 93 (1990) 3111.
- [9] W.H. Wing, G.A. Ruff, W.E. Lamb and J.J. Spezeski, *Phys. Rev. Letters* 36 (1976) 1488.
- [10] A. Carrington, J.A. Buttenshaw, R.A. Kennedy and T.P. Softely, *Mol. Phys.* 45 (1982) 747.
- [11] J.T. Moseley, in: *Advances in chemical physics*, Vol. 60, eds. I. Prigogine and S.A. Rice (Wiley-Interscience, New York, 1985).
- [12] D.M. Neumark, K.R. Lykke, T. Andersen and W.C. Lineberger, *J. Chem. Phys.* 83 (1985) 4364.
- [13] T.A. Miller and V.E. Bondybey, eds. *Molecular ions: spectroscopy, structure and chemistry* (North-Holland, Amsterdam, 1983); R.J. Saykally, *Science* 239 (1988) 157; J.P. Maier, ed., *Ion and cluster ion spectroscopy and structure* (Elsevier, Amsterdam, 1989).
- [14] R.D. Mead, K.R. Lykke, W.C. Lineberger, J. Marks and J.I. Brauman, *J. Chem. Phys.* 81 (1984) 4883.
- [15] J. Marks, J.I. Brauman, R.D. Mead, K.R. Lykke and W.C. Lineberger, *J. Chem. Phys.* 88 (1988) 6785.
- [16] K.R. Lykke, D.M. Neumark, T. Andersen, V.J. Trappa and W.C. Lineberger, *J. Chem. Phys.* 87 (1987) 6842; J. Marks, D.M. Wetzel, P.B. Comita and J.I. Brauman, *J. Chem. Phys.* 84 (1986) 5284.
- [17] T. Andersen, K.R. Lykke, D.M. Neumark and W.C. Lineberger, *J. Chem. Phys.* 86 (1987) 1858.
- [18] U. Hefter, R.D. Mead, P.A. Schultz and W.C. Lineberger, *Phys. Rev. A* 28 (1983) 1429.
- [19] J.L. Hall and S.A. Lee, *Appl. Phys. Letters* 29 (1976) 367.
- [20] L.F. DiMauro, M. Heaven and T.A. Miller, *J. Chem. Phys.* 81 (1984) 2339.
- [21] G. Herzberg, *Electronic structure of polyatomic molecules* (Van Nostrand, New York, 1966).
- [22] J.K.G. Watson, in: *Vibrational spectra and structure*, Vol. 6, ed. J.R. Durig (Elsevier, Amsterdam, 1977).
- [23] R.W. Wetmore, H.F. Schaefer III, P.C. Hiberty and J.I. Brauman, *J. Am. Chem. Soc.* 102 (1980) 5470.
- [24] R.M. Lees and J.G. Baker, *J. Chem. Phys.* 48 (1968) 5299.
- [25] T. Oka and Y. Morino, *J. Mol. Spectry.* 6 (1961) 472; 8 (1962) 9.